Novel simulation approaches for cyclic-steady-state fixed-bed processes exhibiting sharp fronts and shocks

F. Platte, D. Kuzmin, Ch. Fredebeul, S. Turek

Abstract

Over the past decades, the field of chemical engineering has witnessed an increased interest in unsteady-state processes. Multifunctional, as well as intensified chemical processes, may exhibit instationary behaviour especially when based on periodical operating conditions. Ideally, instationary processes lead to a higher yield and increased selectivities compared to conventional steady-state fixed-bed processes. Typical candidates among these are the reverse-flow-reactor, the chromatographic reactor and the adsorptive reactor. Since the underlying regeneration strategy is nearly always based on cycles – e.g. a reaction cycle is followed by a regeneration cycle and so on – the overall temporal behaviour of such processes eventually develops into cyclic steady states (after a transient phase). Experiments reveal a slow transient behaviour into the cyclic steady-state. This can also be observed in simulation based on conventional numerical treatment such as the method of lines. In addition to this problem many instationary processes exhibit sharp fronts or even shocks which require stabilisation of the convective terms. In this work we present a method of combining the idea of global discretisation with modern stabilisation techniques of type FEM-FCT and FEM-TVD in order to obtain an efficient, well approximating and robust tool for the general simulation of instationary and in particularly cyclic-steady-state processes.

1 Instationary fixed-bed processes

Fixed-bed reactors are suggested for many chemical engineering applications. In contrast to batch processes, fixed-bed processes offer the possibility (over the length of the apparatus) of taking influence on the physical processes and chemical reactions inside – in order to obtain higher overall performance. Very often, it is the goal to achieve higher yield and selectivities based on the value product, larger space-time-yield and – in the case of exothermic reactions – to guarantee better heat-integration. Depending on how these modifications are made, one

has to distinguish between intensified and multifunctional processes. In multifunctional reactors (beside the reaction itself) additional process functions, e.g. mixing/separation and/or heat-accumulation are integrated in the apparatus, whereas intensified processes are justified on the fact that most chemical engineering processes are rather limited by heat and mass transport or thermodynamics and not so much by the reaction itself. Hence, intensified as well as multifunctional processes, lead to higher product quality and purity making them economically preferable.
More recently, instationary processes moved into the focus of chemical engineering. This instationary behaviour results from internal or external recursion of heat and/or mass within the process. From the operator's point of view, continuous instationary variants are the most interesting.
In general, one can distinguish between forced-cyclic and autonomous-instationary processes. In both of these, one can monitor moving temperature and concentration fronts which follow reoccurring patterns of cycles after the start-up phase. Multifunctional and intensified processes are either inherently instationary or forced instationary. Their behaviour based on properly chosen operating conditions allow for additional enhancement of the performance. Moreover, the time dependent behaviour leads to more data which can be exploited for model evaluation. Unfortunately, due to the non-linearity and stiffness of many of these instationary fixed-bed processes, experiments and simulations are rather time-consuming projects.

1.1 Application examples

In the following section, three examples of instationary fixed-bed processes are briefly described:

- Example I: Catalytic combustion in reverse-flow operation
- Example II: Adsorptive reactor
- Example III: Coupled endothermic/exothermic reaction in reverse-flow operation

For each example, we present a schematic view of the process function and consider a typical balance (transport) equation either for energy or mass of type

'ACCUMULATION' + 'CONVECTION' = 'DIFFUSION' + 'REACTION' + 'SOURCES/SINKS'.

Then, in each equation we highlight the term that causes numerical instabilities and discuss appropriate numerical treatments.

Example I: Catalytic combustion in reverse-flow operation
One important instationary process is the reverse-flow-reactor (RFR) which is operated in a forced periodical way by switching the side/direction of the inflow (cf. Fig. 1) [14]. One of the most notable advantages of the reverse-flow concept is certainly that due to the regenerative heat recovery, a hot reaction zone surrounded by two cold zones is trapped in the centre of the fixed-bed. The classical RFR operates with two identical half-cycles, i.e. the two functions 'reaction' and 'regeneration' are fulfilled simultaneously. Due to an inherently low heat-loss, even weak exothermic processes (or alternatively processes with trace gases) can remain ignited without additional external heat or fuel gas. Suggested examples for industrial application are the catalytic treatment of waste gases in air, oxidation of SO_2 [15] and many more [16].

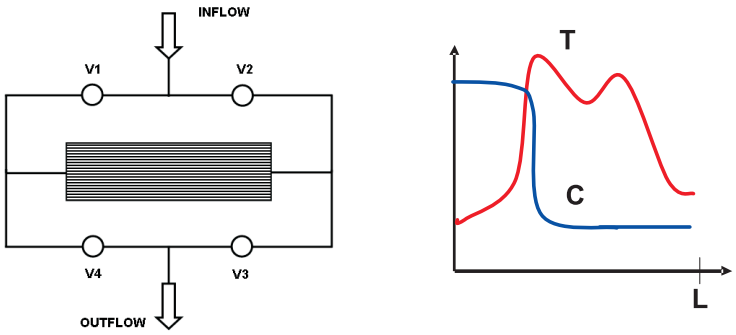

Figure 1: Scheme of a reverse-flow reactor: Cyclic opening and closing of the valves-pairs V1/V3 and V2/V4 (left). Typical temperature-fronts and concentration-distribution within the fixed-bed for a fixed time (right).

Numerical demands for catalytic combustion in reverse-flow operation:
It is well known that the RFR reaches the cyclic-steady-state after a long operation time and a large number of flow-reversals. Moreover, high reaction rates at elevated temperature levels lead to sharp fronts in the distribution of temperature and concentration. Therefore, the numerical algorithms should incorporate a direct calculation of cyclic steady-states and an appropriate stabilisation of the convective terms. High reaction rates in the energy equation (1) may cause sharp profiles.

$$(\varrho c_p)\cdot\frac{\partial T}{\partial t}+\varepsilon_F\varrho c_p\frac{\partial(w_F T)}{\partial z}=\lambda_{ax}\frac{\partial^2 T}{\partial z^2}+\varepsilon_F\underbrace{\sum_j(-\Delta H_{R,i})r_j}_{\text{high reaction rates!}}+\frac{\alpha}{r}(T^*-T)\quad(1)$$

Example II: Adsorptive reactor
The adsorptive reactor is currently considered for enhancing the yield of equilibrium limited reactions. A survey of chemical reactions investigated in gas-phase adsorptive reactors is given in [6]. Fig. 2 illustrates the two functions 'reaction+adsorption' and 'regeneration' in two separate sequential half-cycles. Most of the authors use adsorptive reaction processes as means to enhance equilibrium conversions by the uptake of one of the products according to LE CHATELIER's principle: The equilibrium of the two reactants A and B

$$A + B \Leftrightarrow C + D$$

is shifted to the right hand side. By adsorbing the by-product

$$C \Leftrightarrow C*$$

the conversion of the value product D is increased. Two suggested adsorptive fixed-bed processes can be found in [6].

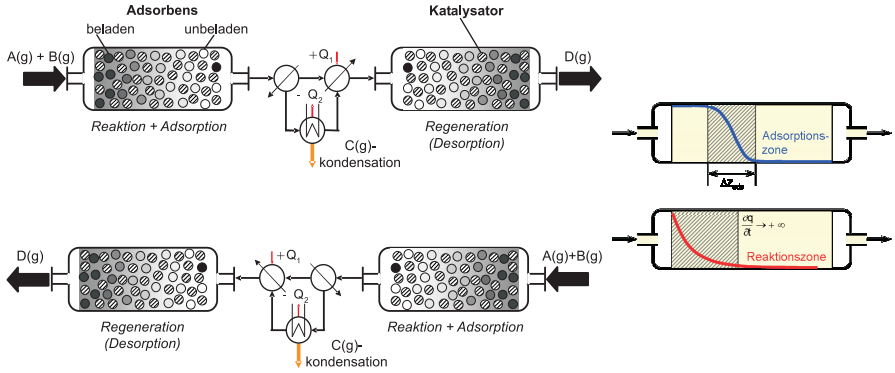

Figure 2: Adsorptive reactor with production- and regeneration-cycle (left) and typical shifted fronts (right) within the cycle.

Numerical demands for adsorptive reactor: Nonlinear adsorption isotherms could cause problems during the calculation due to steep gradients. For example convex isotherms $q(C)$ lead to a so-called self-sharpening effect noticeable in the concentration profiles. In the mass balance (2) one can locate the non-linear accumulation term. Therefore, the numerical algorithms should consider an appropriate stabilisation of the accumulation term.

$$\left(1 + \frac{1-\varepsilon_F}{\varepsilon_F} \cdot \underbrace{\frac{dq(c)^*}{dc}}_{\text{nonlinear accumulation!}}\right) \cdot \frac{\partial c}{\partial t} + w_F \frac{\partial c}{\partial z} = D_{ax} \frac{\partial^2 c}{\partial z^2} + \sum_j \nu_{ij} r_j \quad (2)$$

Example III: Coupled endothermic/exothermic reaction in reverse-flow operation
This example is closely related to example I. Here the reverse-flow operation can also be established by switching the inflow direction. But in contrast to example I, two consecutive half-cycles now fulfil different functions, namely 'endothermic reaction' and 'exothermic regeneration'.

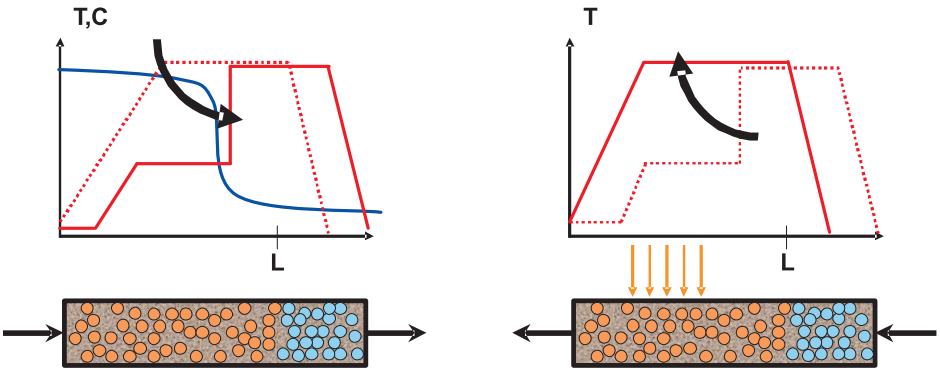

Figure 3: Schematic view of Coupled reaction in RFR: Function of endothermic (left) and exothermic half-cycle (right). Dotted lines denote the distribution at the beginning of each half-cycle. Full lines show where the distributions end up.

Numerical demands for Coupled endothermic/exothermic reaction in reverse-flow operation: Nonlinear equilibrium may cause numerical problems during the calculation due to shock fronts. In the heat balance (3) one can locate the non-linear convective term. Therefore, the numerical algorithms should consider an appropriate stabilisation of the convective terms.

$$\left(\varrho^* c_p^* + \varepsilon_F \varrho c_p\right) \cdot \frac{\partial T}{\partial t} + w_F \varrho c_p \left(1 + \Delta T_{ad} \cdot \underbrace{\frac{dX(T)}{dT}}_{\text{nonlinear convection!}} \right) \frac{\partial T}{\partial z} = \lambda_{ax} \frac{\partial^2 T}{\partial z^2}. \tag{3}$$

In conclusion, for all three presented processes the numerical algorithms must account for

- direct calculation of cyclic-steady-states and
- stabilisation of convective terms.

2 Numerical treatment

Compared to batch-processes, stationary fixed-bed processes are in general more complex to design and to build. Nevertheless, the mathematical description of these two process classes is of similar complexity. In the case of batch processes, one has to appropriately handle (large) systems of time-dependent ODEs, whereas stationary fixed-bed processes cause difficulties due to the spatial distribution of the variables. Comparing stationary and instationary processes leads to a similar conclusion: The additional temporal behaviour implies stronger demands on the experimental equipment and the operation of such apparatus. From the mathematical point of view, chemical engineers are still commonly tackling these problems by discretising the analytically insolvable PDEs in spaces and then integrating the resulting ODE-system in time. This method is referred as method-of-lines (mol). Unfortunately, this approach suffers very often from slow transient behaviour due to the nonlinear nature and stiffness of the problem. It should be stressed that modern time-integrators – based on multi-step or extrapolation schemes – which allow for large time steps, lose most of their efficiency after every switch. Strictly speaking, a new initial value problem arises and for reasons of accuracy and stability most algorithms start over with a one-step scheme, e.g. an implicit one-step Euler scheme in combination with a small time step. Additionally, the exact transient behaviour into the cyclic-steady-state is not of major interest for a systematic process-design (cf. Fig. 4). For the analysis, design and optimisation of instationary processes one merely requires knowledge of cyclic-steady-states. When using conventional dynamical simulations, sometime up to a few hundred cycles need to be simulated [21]. On the other hand, due to the inherently instationary behaviour one cannot find steady-state solutions by just setting the time-derivatives to zero and solving the resulting system. This becomes clear when looking at a typical (cf. Fig. 4, middle) behaviour in time.

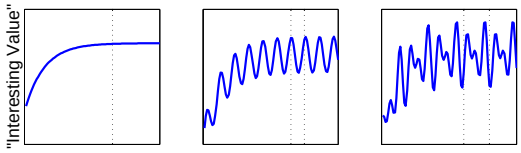

Figure 4: Principle transient behaviour of a stationary, (cyclic) instationary and chaotic processes (left to right)

For the direct calculation of cyclic-steady-states modern algorithms make use of the periodicity condition, such as symmetries of the solution at the beginning and the end of full cycle. As a result, the problem is reformulated from an initial value problem (IVP) to a (stationary) boundary value problem (BVP) in space and time which can consequentially be solved e.g. by the shooting method or by a global discretisation over a period. We have restricted our research to latter.

2.1 Space-time finite-difference discretisation

An efficient approach to solve the governing equations is the direct calculation method which can be based on global discretisation. Alternatively, a direct calculation of cyclic-steady-states can be solved with a dynamical simulation wrapped by a shooting method algorithm. Both methods exhibit characteristic advantages. We choose the global discretisation approach since we believe that it allows better implementation of modern mathematical algorithms (mesh-generation, discretisation and solvers) developed for 2D/3D problems, whereby the shooting method is essentially restricted to method of lines.

Earlier research clearly shows that either approach is far more efficient than a simple dynamical simulation – but only when cyclic steady-states are of major interest [21, 22]. In particular, this applies to the case of parameter studies in which hundreds of cyclic steady-states must be calculated. To obtain a well posed problem, in addition to the usual Danckwerts boundary conditions in space, we require either an initial value condition or boundary value conditions in time. A initial value is usually a prescribed distribution, e.g. of the temperature

$$T(z, t = 0) = T_0(x).$$

A typical boundary condition in the case of the RFR can be a mirror symmetric profile for the temperature in time:

$$T(z, t) = T(L - z, t + \Delta t_{cyc}).$$

It should be noted that this (mirror) symmetry condition formulated in the direct calculation is precisely the commonly used stopping criterion in the dynamical simulation. Tab. 1 shows a comparison of the two approaches.

Table 1: Comparison of state of the art methods for direct calculation

	Shooting method	**Global discretisation**
memory consumption	moderate	high
flexibility	comparably high	low
stability of iteration	possibly problematic	high
discretisation	adaptive	adaptive
2D/3D	unclear	simple
Stabilising conv. terms	possibly FCT	TVD

2.2 Treatment of convection-dominated cases

There are several general demands on a 'good' numerical algorithm, e.g., high accuracy, robustness and moderate consumption of computer resources. These prerequisites are rather difficult to satisfy for the above-mentioned class of problems due to following effects:

- Strongly exothermic reactions in RFR → **steep gradients**.
- Adsorptive/desorptive reactions → **self-sharpening phenomena**.
- Endothermic/exothermic coupling in RFR → **shock-like fronts**.

In light of the above effects, the direct calculation should be based on a numerical method that provides a proper stabilization of the 'bad-behaved' convective terms. Let us consider a generic transport equation typical of non-stationary processes in a fixed bed reactor

$$a_1 \frac{\partial u}{\partial t} + a_2 \frac{\partial u}{\partial z} = a_3 \frac{\partial^2 u}{\partial z^2} + a_4(u - u^*) + f(u, v, \ldots). \tag{4}$$

It is well known that discretisation of the first derivatives in the left-hand side is a potential source of numerical troubles. Standard high-order methods give rise to non-physical oscillations, while the results produced by low-order ones are corrupted by excessive numerical diffusion. Unfortunately, there is no way out of this dilemma as long as the discretisation technique is **linear** [10]. Therefore, modern high-resolution schemes are typically based on a **nonlinear** approximation of the convective fluxes. Roughly speaking, a high-order method is employed in regions where the solution is sufficiently smooth but in the vicinity of steep gradients it is replaced by a non-oscillatory first-order scheme like 'upwind'. The far-reaching idea of adaptive switching between high- and low-order discretisations can be traced back to the concepts of *flux-corrected transport* (FCT) which were introduced in the early 1970s by Boris and Book [4].
In the limit of pure convection, any physically admissible solution to a scalar transport problem proves *total variation diminishing* (TVD). In one dimension, the total variation is defined as

$$TV(u) = \int \left| \frac{\partial u}{\partial x} \right| dx. \tag{5}$$

As long as this quantity does not increase with time, it can be shown that

- there is no formation and/or enhancement of local extrema,
- positivity and/or monotonicity of initial data is preserved.

Hence, it is natural to require that numerical solutions also possess these properties, which lead to the following constraint to be imposed at the fully discrete level

$$TV(u^{n+1}) \le TV(u^n), \quad \text{where} \quad TV(u^n) = \sum_i |u_i^n - u_{i-1}^n|. \tag{6}$$

Here and below u_i stand for the values of the approximate solution at the mesh nodes z_i and the superscripts refer to the time level at which it is evaluated.

To illustrate the derivation of classical TVD schemes, consider the linear convection equation

$$\frac{\partial u}{\partial t} + v\frac{\partial u}{\partial z} = 0, \qquad v > 0 \tag{7}$$

discretised in space by a conservative finite difference/volume method which yields

$$\frac{\mathrm{d}u_i}{\mathrm{d}t} + \frac{f_{i+1/2} - f_{i-1/2}}{\Delta z} = 0. \tag{8}$$

The neighbouring grid points x_i and $x_{i\pm1}$ exchange the conserved quantities via numerical fluxes $f_{i\pm1/2}$ which are supposed to be consistent with the underlying continuous flux $f = vu$. Harten [11] proved that such a semi-discrete scheme is TVD if it can be rewritten in the form

$$\frac{\mathrm{d}u_i}{\mathrm{d}t} = c_{i-1/2}(u_{i-1} - u_i) + c_{i+1/2}(u_{i+1} - u_i) \tag{9}$$

with (possibly nonlinear) nonnegative coefficients $c_{i-1/2} \geq 0$ and $c_{i+1/2} \geq 0$. To meet these requirements, the numerical flux for a TVD method can be constructed by blending a high-order approximation $f^H_{i+1/2}$ and its low-order counterpart $f^L_{i+1/2}$ as follows

$$f_{i+1/2} = f^L_{i+1/2} + \Phi_{i+1/2}[f^H_{i+1/2} - f^L_{i+1/2}], \qquad 0 \leq \Phi_{i+1/2} \leq 2, \tag{10}$$

where the value of $\Phi_{i+1/2}$ depends on the local smoothness of the solution and on the choice of the **limiter** function. If the linear flux approximations are given by

$$f^L_{i+1/2} = vu_i \qquad \text{and} \qquad f^H_{i+1/2} = v\frac{u_{i+1} + u_i}{2}, \tag{11}$$

then it is easy to verify that the standard upwind, central, and downwind discretisation of the convective term are recovered in case of $\Phi_{i+1/2} = 0, 1,$ and 2, respectively. The most popular flux limiters are known as MINMOD, VAN LEER, MC, and SUPERBEE. All of them yield non-oscillatory results but their numerical behaviour may be quite different. For a detailed presentation and a comparative study of classical TVD methods, the interested reader is referred to [24].

A fully multidimensional flux limiter of TVD type was proposed by Kuzmin and Turek [12]. Their novel approach to the design of high-resolution schemes is based on the principle of *algebraic flux correction*. In essence, a centred space discretisation of the convective terms is rendered *local extremum diminishing* (LED → TVD in the 1D case) by a conservative elimination of negative off-diagonal coefficients from the discrete operator. This straightforward 'postprocessing' technique is very flexible and can be readily integrated into existing CFD codes.

The flow chart of required algebraic manipulations is sketched in Fig. 5. First, the governing equation is discretised in space by an arbitrary linear high-order method (e.g. central differences or the Galerkin FEM) which yields a system of ordinary differential equations for the vector of time-dependent nodal values. In the

finite element context, the consistent mass matrix M_C is replaced by its 'lumped' counterpart M_L. Furthermore, the high-order transport operator K is transformed into a non-oscillatory low-order one by adding a *discrete diffusion operator* D (i.e., a symmetric matrix with zero row and column sums) designed so as to get rid of all negative off-diagonal coefficients. In order to prevent excessive smearing, it is necessary to remove as much artificial diffusion as possible without generating wiggles. To this end, a limited amount of compensating *antidiffusion* F is added in the next step. In practice, both diffusive and antidiffusive terms are represented as a sum of internodal fluxes which are constructed edge-by-edge and inserted into the global vectors. Even though the final transport operator K^* does have negative off-diagonal coefficients, they are harmless as long as there exists an equivalent LED representation of the modified scheme. That is: for a given solution vector u, there should exist a matrix L^* such that all off-diagonal entries l_{ij}^* are nonnegative and $L^*u = K^*u$.
Remarkably, this methodology is directly applicable to steady-state problems as well as to time-dependent PDEs reformulated as stationary ones in space-time domain. To put it another way, it is possible to solve the discretised equations for

1. Linear high-order scheme (e.g. Galerkin FEM)

$$M_C \frac{\mathrm{d}u}{\mathrm{d}t} = Ku \quad \text{such that} \quad \exists\, j \neq i:\ k_{ij} < 0$$

2. Linear low-order scheme $L = K + D$

$$M_L \frac{\mathrm{d}u}{\mathrm{d}t} = Lu \quad \text{such that} \quad l_{ij} \geq 0,\ \forall j \neq i$$

3. Nonlinear high-resolution scheme $K^* = L + F$

$$M_L \frac{\mathrm{d}u}{\mathrm{d}t} = K^*u \quad \text{such that} \quad \exists\, j \neq i:\ k_{ij}^* < 0$$

Equivalent representation $L^*u = K^*u$ is LED

$$M_L \frac{\mathrm{d}u}{\mathrm{d}t} = L^*u \quad \text{such that} \quad l_{ij}^* \geq 0,\ \forall j \neq i$$

Figure 5: Roadmap of matrix manipulations.

all time levels simultaneously instead of doing it step-by-step as usual. Consider a scalar conservation law discretised in space and time by a linear second-order scheme (e.g., central differences / leapfrog time-stepping)

$$M_L \frac{u^{n+1} - u^{n-1}}{2\Delta t} = Ku^n, \qquad n = 2, \ldots, M \tag{12}$$

where $u^n = [u_1^n, \ldots, u_N^n]^T$ denotes the vector of nodal values at the time level $t^n = (n-1)\Delta t$.
Combining the $N \times M$ equations, we obtain an algebraic system of the form $Au = f$, where

$$A = \begin{bmatrix} -M_L - \Delta tK & M_L & & & & \\ -M_L & -2\Delta tK & M_L & & & \\ & -M_L & -2\Delta tK & M_L & & \\ & & \cdots & \cdots & & \\ & & -M_L & -2\Delta tK & M_L & \\ & & & -M_L & M_L - \Delta tK \end{bmatrix}, \qquad u = \begin{bmatrix} u^1 \\ u^2 \\ u^3 \\ \cdots \\ u^{M-1} \\ u^M \end{bmatrix}. \tag{13}$$

Since the coefficients of A and K have opposite signs, all **positive** off-diagonal ones need to be eliminated. If the order of nodes is such that $a_{ji} < a_{ij}$, then the 'optimal' artificial diffusion coefficient is given by $d_{ij} = \max\{0, a_{ij}\}$ [12]. The required matrix modification is as follows:

$$\begin{aligned} a_{ii} &:= a_{ii} + d_{ij}, \qquad & a_{ij} &:= a_{ij} - d_{ij}, \\ a_{ji} &:= a_{ji} - d_{ij}, \qquad & a_{jj} &:= a_{jj} + d_{ij}. \end{aligned}$$

As a result, we obtain a non-oscillatory low-order operator which has no positive off-diagonal entries and no negative diagonal ones (a so-called *M-matrix*)

$$A^* = \begin{bmatrix} -\Delta tL & 0 & & & & \\ -2M_L & 2M_L - 2\Delta tL & 0 & & & \\ & -2M_L & 2M_L - 2\Delta tL & 0 & & \\ & & \cdots & & & \\ & & -2M_L & 2M_L - 2\Delta tL & 0 & \\ & & & -2M_L & 2M_L - \Delta tL \end{bmatrix}. \tag{14}$$

Here L represents the least diffusive linear LED counterpart of K [12]. Interestingly enough, the fully implicit upwind difference scheme is recovered in the case of pure convection in 1D.
The converged low-order solution serves as a reasonable initial guess for the space-time TVD solution to be computed in an iterative way within an outer defect correction loop. Each defect/flux correction cycle consists of the following algorithmic steps [12]

1. Compute the residual of the low-order scheme $r = f - Au$.
2. Evaluate the limited *antidiffusive fluxes* $f_{ij}^a = \Phi_{ji} d_{ij}(u_i - u_j)$ and insert them into the global defect vector r, see [12] for details.
3. Solve the linear sub-problem $A\Delta u = f$ and compute $u := u + \Delta u$.

All the necessary information is extracted from the original matrix A, while its low-order counterpart A^* constitutes an excellent preconditioner. In each outer iteration, the quality of the solution improves but intermediate results may exhibit spurious undershoots/overshoots. In order to secure the convergence, it is worthwhile to perform implicit underrelaxation (divide the diagonal entries of the preconditioner by a suitably chosen parameter $0 < \omega \leq 1$ so as to enhance the diagonal dominance) which can be interpreted as a local time-stepping method [7].

3 Numerical results

3.1 Prestudy: Cauchy problem

As a prestudy a pure transport problem was considered (15). A step (initial value) moves with a constant positive velocity of 0.5 in space:

$$u_t + 0.5 \cdot u_x = 0 \qquad (x,t) \in \Omega = (0,1)^2, \tag{15}$$

$$u(z, t=0) = \begin{cases} 0, & \text{for} \quad 0.0 \leq z \leq 0.2 \\ 1, & \text{for} \quad 0.2 < z < 0.4 \\ 0, & \text{for} \quad 0.4 \leq z \leq 1.0 \end{cases}$$

Although there is an analytical solution for this problem, the numerical treatment is very hard to solve due to the two discontinuities. Therefore, this Cauchy-problem is an adequate test for the quality of the numerical method. The computational domain was chosen to be a unit-square. An equidistant mesh comprising 100 points in time and 50 in space was applied which corresponds to 5000 as overall number of unknowns. The global discretisation was based on the leapfrog-scheme (LF) which tends to exhibit unacceptable oscillations for non-smooth solutions

$$\frac{u_i^{j+1} - u_i^{j-1}}{2\Delta t} + v \frac{u_{i+1}^j - u_{i-1}^j}{2\Delta z} = 0$$

and hence, results in a system of linear algebraic equations

$$M^{LF}\mathbf{U} = b. \tag{16}$$

The nodal unknowns u_i^j for $i = 1, \ldots, 1/\Delta z - 1$ and $j = 1, \ldots, 1/\Delta t - 1$ approximate the solution of (15) in the points (z_i, t^j) for $z_i = i \cdot \Delta z$ and $t^j = j \cdot \Delta t$. The matrix

M^{LF} depicts the so-called discrete transport operator and the right hand side b contains the initial condition (step) and spatial boundary conditions. Solving the linear system (16) directly by any linear solver, e.g. by direct solvers, leads to a solution exhibiting the mentioned oscillations throughout the domain (cf. Fig.6, left). To suppress these numerical or unphysical oscillations and to present the power of non-linear stabilisation techniques we applied the FEM-TVD method suggested by Kuzmin and Turek [12]. Starting from the linear system (16), this method first substitutes the high order transport operator by the help of *discrete upwinding*. The new transport matrix M^{DU} already fulfils TVD-properties but it is also very diffusive at the same time (cf. Fig.6, middle). Secondly, in a defect-correction-loop the amount of additional admissible antidiffusive flux for each node is detected by the help of limiter functions and then added nodewise. By this measure the solution can essentially be extended to second order accuracy and still fulfilling TVD properties at the same time. This correction is carried out in the right hand side vector to prevent a costly matrix update in each step (cf. previous section). Fig.6 shows a considerable low amount of numerical diffusion in the plotted solution vector. (In this case the SUPERBEE-limiter function was chosen which leads to extreme low numerical diffusion.)

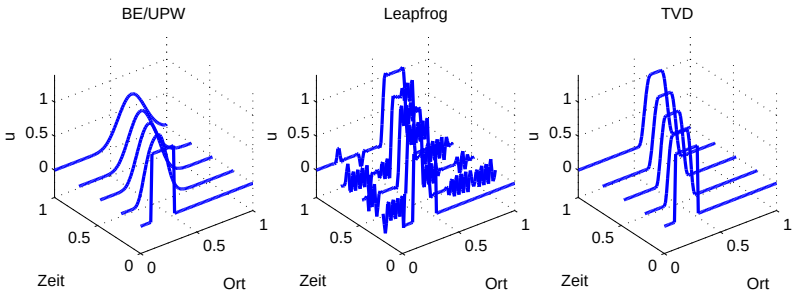

Figure 6: Pure transport of a step. Solved with upwinding (left), non-stabilised *Leap-frog* (middle) and space-time-TVD (right)

3.2 Catalytic combustion of N_2O in reverse-flow operation

In the case of the catalytic combustion of N_2O in reverse-flow operation we are also able to compare our simulations with experimental results retrieved from our laboratory of Bio- and chemical engineering [17]. Looking at Fig.7 one can find a qualitative good agreement of calculated and measured temperature profiles. It can clearly be seen that the non-adiabatic condition leads to heat losses forming 'M'-shaped temperature profiles. Although the reaction rates are quite large there was no need for the application of TVD-stabilisation. In the present case, the convective terms were discretised and sufficiently solved by a linear LUDS approach [24].

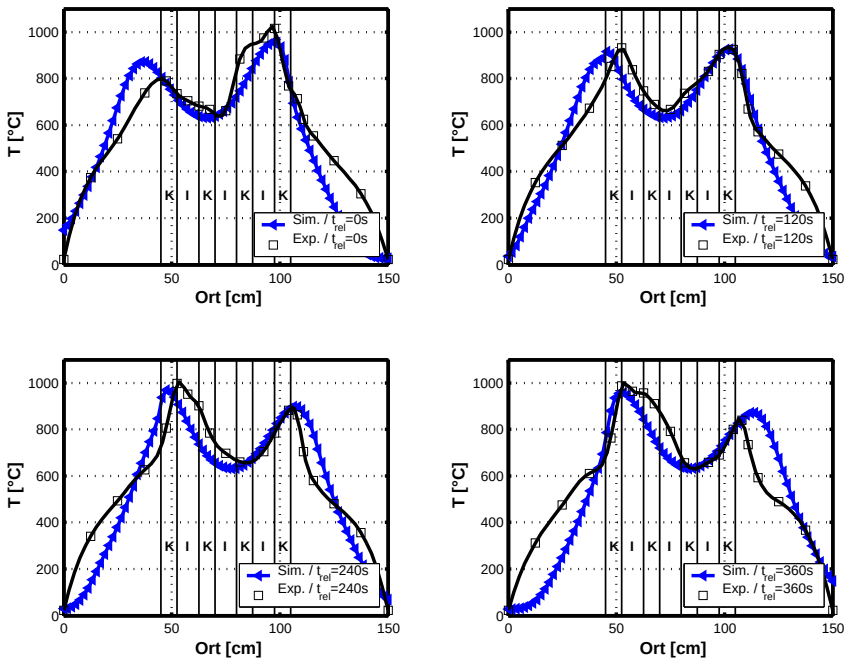

Figure 7: Comparison between simulation and experiment. Four spatial temperature distributions at four time-points within the cycle are depicted. The measured 'M'-shaped profiles and the local extrema are qualitatively well predicted by the direct calculation. Cycle-time is $\Delta t_{cyc} = 180s$ and inlet is concentration $C = 2,0$ mol/m^3.

3.3 Endothermic steam reforming in reverse-flow operation

To present the power of the implemented TVD-algorithms not only for the test case, but also for a technically relevant problem, we now consider a novel fixed-bed process for the methane-steam-reforming under instationary conditions, most recently suggested in [9]. Here only the reaction cycle was simulated from which it is known that it can exhibit shock fronts. In [9] a simplified model is derived under the assumption that the reaction dominates, compared to any physical diffusion of mass and heat. The resulting model consists only of one heat balance

$$\left((1-\varepsilon)\varrho^* c_p^*\right) \cdot \frac{\partial T}{\partial t} + \dot{m} c_p \left(1 + \Delta T_{ad} \frac{dX(T)}{dT}\right) \frac{\partial T}{\partial z} = 0. \tag{17}$$

The crucial part for the simulation is the knowledge of the temperature dependent equilibrium $X(T)$. In [9] this function was found to exhibit a saturating behaviour. For low temperatures X adopts values just above zero increasing fast around 800

K and then approaching the unity for higher temperatures which thermodynamically corresponds to nearly full conversion of the (value) product. In this case the equilibrium function shows an inflexion point at approx. 820 K. As a result the first derivative $dX(T)/dT$ possesses an extreme value (maximum) at the same temperature. With respect to the simplified model (17) one can find the derivative $dX(T)/dT$ incorporated in the convective term which leads to the mentioned shock fronts. We also applied a global discretisation based on the leap-frog stencil for this problem. All physical properties were taken from [9]. The computational rectangular domain has the size $0 \leq z \leq 0.7$ for the space coordinate in meters and the size $0 \leq t \leq 60$ for the time in seconds. We choose 200 grid points in each dimension. For the initial temperature distribution, T(t=0,z), we selected a ramp which graduately increases from 400 to 1500 K in the first 10 cm and then remains constant at 1500 K (cf. Fig. 8, right, first line).

$$T(z, t=0) = \begin{cases} 400 + 11000 \cdot z, & \text{for} \quad 0.0 \leq z \leq 0.1 \\ 1500, & \text{for} \quad 0.1 \leq z \leq 0.7 \end{cases} .$$

This initial condition enables shocks to develop because there are temperatures lower and higher than 820 K. Since only the first half-cycle (reaction cycle) was considered there was no need to formulate periodicity conditions in time. Hence the calculation is more of a dynamical simulation – but in which all time steps are simultaneously solved – than a true direct calculation. The presented test case can be regarded as worst-case approximation as the model equation includes no physical diffusion at all. With some justification it can be claimed that any amount of additional diffusion in the physical model will lead to better convergence behaviour in the nonlinear solution loop.

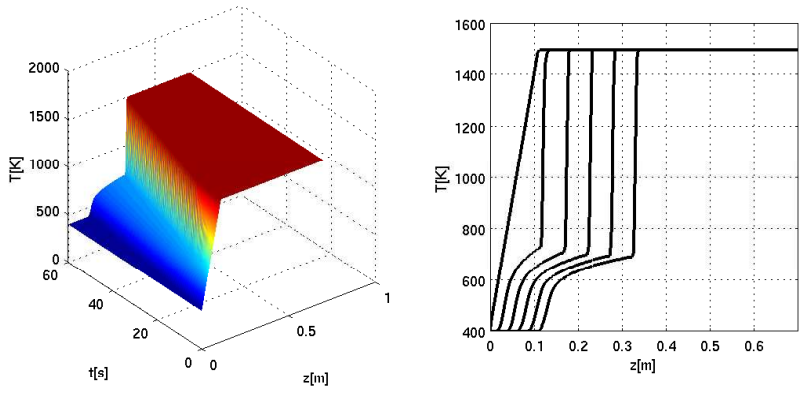

Figure 8: Thermodynamically determined endothermic reaction forms shocks

With respect to Fig. 8 one can clearly see the formation of the shock front in the temperature distribution during the course of the cycle. The solution profiles exhibit a considerable low amount of diffusion so that the gradients are resolved very accurately.

Numerical behaviour
From the three presented test cases it can be concluded that the global discretisation in combination with stabilisation techniques for convective dominated transport problems delivers a flexible and accurate numerical treatment of the underlying mathematical model. But is the method also efficient and fast? To tell the truth there are still unresolved numerical problems. The sharper the fronts become the more non-linear iterations must be carried out in order the bring the residual close to zero. In our future work we shall focus on an appropriate treatment of the non-linear flux correction in the TVD algorithm. These could for example be based on pseudo time-stepping or methods of quasi-Newton type.

4 Summary and discussion

Many intensified and multifunctional fixed bed processes in the field of chemical engineering exhibit cyclic-steady-states due to the underlying operation scheme – reaction cycle followed by regeneration cycle and so on. Since standard numerical simulations based on method of lines reach the cyclic-steady-state only after a long simulation time and many simulated cycles, modern numerical methods for the direct calculation of cyclic-steady-states have attracted an increased interest. In particularly in the case of parameter studies, where many cyclic-steady-states are to be calculated, this approach is a must. We have presented a modified direct calculation which is based on space-time global discretisation of the governing model equations. This technique enables the user to calculate initial value problems as well as boundary value problems. In addition to this, modern non-linear stabilisation techniques of type FEM-TVD have been incorporated. This way not only sharp fronts are resolved with a high accuracy, but also shocks do not lead to a break-down of calculation.

Acknowledgement: This work became possible due to funding of Deutsche Forschungsgemeinschaft (DFG). Special thanks belong to R.Dyll.

References

[1] Agar, D.W., Galle, M., Watzenberger, O., 2001, Thermal N_2O Decomposition in Regenerative Heat Exchanger Reactors. *Chem. Ing. Sci.*

[2] Baerns, M., Hofmann, H., Renken, A., 1987, Chemische Reaktionstechnik - Lehrbuch der Techischen Chemie, Band **1 15**.

[3] Björck, A., Dahlquist, G., 1972, Numerische Methoden. *R. Oldenbourg Verlag, München* **Auflage 1**.

[4] Boris, J.P. and Book, D.L., 1973, Flux-corrected transport. I. SHASTA, A fluid transport algorithm that works. *J. Comput. Phys.* **11** 38–69.

[5] Davis, T.A., Duff, I.S., 1997, *A Combined Unifrontal/Multifrontal Method for unsymmetric Sparse Matrices*, Technical Report TR-97-016, Computer and Information Science and Engineering Department, University of Florida

[6] Elsner, M.P., Dittrich, C., Agar,D.W., 2002, Adsorptive reactors for enhancing equilibrium gas-phase reactions Two case studies Chemical Engineering Science 57 (9), 1607

[7] Ferziger J.H., and Peric, M.,1996, *Computational Methods for Fluid Dynamics*. Springer.

[8] Galle, M., 2001, Hybride homogene und heterogene Reaktionsführung in Hochtemperatursystemen am Beispiel der Lachgaszersetzung, *Dissertation, University of Dortmund*

[9] Glöckler, B., Kolios, G., Eigenberger, G., 2003, Analysis of a novel reverse-flow reactor concept for autothermal methane steam reforming, *Chem. Eng. Sci.* **58**. 593-601

[10] Godunov, S.K., 1959, Finite difference method for numerical computation of discontinuous solutions of the equations of fluid dynamics. *Mat. Sbornik* **47** 271-306.

[11] Harten, A., 1983, High resolution schemes for hyperbolic conservation laws. *J. Comput. Phys.* **49** 357–393.

[12] Kuzmin, D. and Turek,S., 2004, High-resolution FEM-TVD schemes based on a fully multidimensional flux limiter. *J. Comput. Phys.* **198** 131-158.

[13] Kuzmin, D., Möller, M. and Turek, S., 2004, High-resolution FEM-FCT schemes for multidimensional conservation laws. Submitted to *Comput. Methods Appl. Mech. Engrg.*

[14] Matros, Yu. Sh., 1989, Catalytic processes under unsteady-state conditions. *Studies of surface Science and catalysis* **43**,. Amsterdam, Elsevier

[15] Matros Yu. Sh., Boreskov, G. K., Lahmostov, V. S., Volkov, Yu. V., & Ivanov, A. A., 1984, *Method of producing sulfur trioxide.* US Patent 4,478,808.

[16] Matros, Yu. Sh., & Bunimovich, G. A., 1996, Reverse-flow operation in fixed-bed catalytic reactors. *Catalysis Review-Science and Engineering,* 38, 1-68.

[17] Nalpantidis, K., 2003, Untersuchung der heterogen/homogen Zersetzung von N_2O in einem periodisch betriebenen Festbettreaktor, *Diploma thesis, University of Dortmund*

[18] Platte, F., 2000, Untersuchungen zum nichtlinearen dynamischen Verhalten des Reverse Flow Reactors im Hinblick auf die Diskriminierung gekoppelter homogener und heterogener Reaktionsbeiträge bei der N_2O-Zersetzung. *Diploma thesis, University od Dortmund*

[19] Platte, F., Fredebeul, C., 2000, *Dynamische und stationäre Simulation des Reaktionsverhaltens eines Strömungsumkehrreaktors*, Ergebnisberichte Angewandte Mathematik Nr. 190 - T, University of Dortmund

[20] Platte, F., Fredebeul, C., 2001, *Zur Anwendung direkter Löser bei der direkten Berchnung periodisch stationärer Zustände eines Strömungsumkehrreaktors*, Ergebnisberichte Angewandte Mathematik Nr. 197 - T, Uni Dortmund

[21] Salinger, A.G., 1996, The Direct Calculation of Periodic States of the Reverse Flow Reactor - I. Methodology and Propane Combustion Results. *Chem. Eng. Sci.* **51**, 4903-4913

[22] Salinger, A.G., 1996, The Direct Calculation of Periodic States of the Reverse Flow Reactor - II. Multiplicity and Instabiliy. *Chem. Eng. Sci.* **51**, 4915-4922

[23] Seydel, R., 1990, Practical bifurcation and stability analysis - from equilibrium to chaos. *Springer Verlag, New York* **2nd Edition**

[24] Sokolichin, A. 2003, *Mathematische Modellbildung und numerische Simulation von Gas-Flüssigkeits-Blasenströmungen*. Habilitation thesis, University of Stuttgart.

[25] Unger, J., Kolios, G., Eigenberger, G., 1997, On the Efficient Simulation and Analysis of Regenerative Processes in cyclic operation, *Comp. Chem. Eng.* **21**. 167-172

University of Dortmund
Department of Applied Mathematics
Vogelpothsweg 87
D-44221 Dortmund, Germany
Email address: Frank.Platte@math.uni-dortmund.de